

MONTE CARLO METHODS FOR THREE DIMENSIONAL SPIN- $\frac{1}{2}$ SYSTEMS

TERM PAPER REPORT FOR THE COURSE P452

April 26, 2022

Abstract

An important problem in condensed matter physics is how the interactions between electrons in a lattice gives rise to properties like magnetism. Classically, the electrons in a solid is modelled by a lattice of classical spins \mathbf{S}_i which are taken as unit vectors in the three dimensional space, \mathbb{R}^3 , or the Heisenberg model. The Hamiltonian accounts for the interaction between the electrons and also with an external magnetic field (if one is applied). As a part of the term paper assignment, a magnetic material is modelled using Monte Carlo methods.

1 Introduction

Methods of simulating classical many-particle systems based on (pseudo-)‘random’ numbers are called Monte Carlo methods, after the famous Mediterranean casino town. In addition to studying classical many-particle systems, *Monte Carlo methods* can also be used to study quantum problems which involve many particles — for example, calculating the expectation value of the magnetic properties of matter. Use of the *Metropolis algorithm* along with *Monte Carlo* methods allows one to generate a sequence of distributions of a system, or a so-called *Markov chain*. This distribution of the configurations can be used to estimate the static and dynamic properties of classical and quantum many-particle systems.

2 Machinery for Monte Carlo Method

Monte Carlo methods utilises a sequences of (pseudo-)random numbers to perform the simulation. In Monte Carlo methods, the physical process under study, is simulated directly. For modelling spin- $\frac{1}{2}$ systems in matter, writing down the differential equations describing the behaviour of the system is not even required if Monte Carlo methods are used. The sole requirement is that the probability distribution function describing the physical system must be known, the Monte Carlo simulation runs by random sampling from the chosen probability distribution function [3].

How good a Monte Carlo simulation is depends on the selection of random states, or numbers, according to the chosen probability distribution. Monte Carlo simulations use algorithms based on Markov processes to generate random states. A *Markov process* is a random walk with a selected probability for making a move[5], independent of the previous moves. Markov chains, when allowed to be run for a long enough time, is most likely to have reached majority of the states of the system, hence it is *ergodic*.

2.1 High-dimensional Integrals: Monte Carlo Integration

For an integral in, say n variables, $R = r_1, r_2, \dots, r_n$, the integral in higher dimensions would be written as

$$I = \int_D F(R) dR$$

The Monte Carlo method can be used as a stochastic method for integration using random variables, for *any* number of dimensions. The integral can be evaluated using a Monte Carlo method as

$$I \approx \sum_{i=1}^m w_i F(R_i)$$

where w_i are the weights determined by the distribution of the random numbers R_i . If the points at which the function $F(R)$ is evaluated are uniformly distributed, then the integral is

$$I \approx \frac{1}{m} \sum_{i=1}^m F(R_i)$$

where m points have been sampled from the domain D of the integral following the probability distribution function $\mathcal{W}(R)$. Despite a slow convergence rate, $\mathcal{O}(1/\sqrt{m})$, Monte Carlo methods to evaluate integrals in higher dimensions is quite efficient.

2.2 Generating configurations and Sampling Metropolis Algorithm

The *Metropolis algorithm* is a Markov chain Monte Carlo method used for sampling from multi-dimensional distributions. Direct sampling to obtain a sequence of random samples with a probability distribution $P(x)$ is difficult, because calculating the normalisation factor so that $\int_D P(x)dx = 1$ is extremely difficult in most cases.

In the Metropolis algorithm, the random samples is drawn from a distribution $f(x) \propto P(x)$. The requirement that $f(x)$ has to be only proportional to $P(x)$ rather than being exactly equal removes the requirement of calculating the normalisation factors. For a reversible Markov process, using the principle of detailed balance

$$P(i)W(i \rightarrow j) = P(j)W(j \rightarrow i)$$

where $P(i)$ is the probability of the state i and $W(i \rightarrow j)$ is the transition probability from the state i to the state j . In most situations, the transition probability $W(i \rightarrow j)$ is not known. In the Metropolis algorithm, $W(i \rightarrow j)$, can be written as the product of the two probabilities, the probability of accepting the trial move from state i to state j $A(i \rightarrow j)$ and the probability of making a transition to state i to state j $T(i \rightarrow j)$.

$$W(i \rightarrow j) = T(i \rightarrow j)A(i \rightarrow j)$$

At equilibrium, the principle of detailed balance gives,

$$\begin{aligned} \frac{P(i)}{P(j)} &= \frac{W(j \rightarrow i)}{W(i \rightarrow j)} \\ &= \frac{T(j \rightarrow i)A(j \rightarrow i)}{T(i \rightarrow j)A(i \rightarrow j)} \\ \text{or, } \frac{A(j \rightarrow i)}{A(i \rightarrow j)} &= \frac{P(i)T(i \rightarrow j)}{P(j)T(j \rightarrow i)} \end{aligned}$$

For the simplest form of the Metropolis algorithm, the transition probabilities are assumed to be symmetric, $T(i \rightarrow j) = T(j \rightarrow i)$, in which case

$$\frac{A(j \rightarrow i)}{A(i \rightarrow j)} = \frac{P(i)}{P(j)}$$

which gives the ratio of the acceptance probabilities.

Algorithm :

1. Generate a trial c for the next sample based on the current sample value x_i , with transition probability $T(i \rightarrow j)$.
2. Calculate the acceptance ratio $\alpha = \frac{f(c)}{f(x_i)}$ to decide whether to accept or reject the trial move. As $f(x) \propto P(x)$, $\alpha = \frac{f(c)}{f(x_i)} = P(c)/P(x_i)$.
3. Draw a random number $r \in [0, 1]$ from a uniform distribution. If $r \leq \alpha$, accept

the trial move by setting $x_j = c$, else reject the trial move and generate a new trial move.

3 Simulation of spin $\frac{1}{2}$ systems

Monte Carlo methods would be used to simulate the properties of the magnetic material and determine the temperature at which the phase transitions occurs in the system as done in [8], with sampling done using the Metropolis algorithm. For the available computational resources, it has been possible to simulate cubic system with up to 20 lattice points per side in a reasonable amount of time, with periodic boundary conditions will be adopted. The Boltzmann distribution of a spin system is studied to determine the behaviour of the magnetic material for a particular temperature.

For this term paper, results similar to those obtained in [6] would be tried to be generated.

- The total mean energy $\langle E \rangle$ and mean magnetisation per spin $\langle \vec{m} \rangle$ would be recorded for each configuration generated. To determine the expectation values, $\langle E \rangle$ or $\langle \vec{m} \rangle$ a Boltzmann probability distribution is used.

$$P(c_i) = \frac{1}{Z} e^{-\beta E_i}$$

where, $Z = \prod_i \int \left(\frac{d\phi_i d \cos \theta_i}{4\pi} \right) e^{-\beta E_i}$

determines the partition function of the system [6].

- The arrangement of spins before and after the phase transition would be mapped, and the critical temperature, (T_c) , would be attempted to be found out. As described in [8], the critical temperature can be calculated using the fourth order cumulant.

$$U_L = 1 - \frac{1}{3} \frac{\langle m^4 \rangle}{\langle m^2 \rangle^2}$$

with $U_L(T)$ for various sizes of the system intersecting at the critical temperature.

- An attempt would be made to generate the critical exponents as obtained in [8], [6]. It can be shown that at temperatures T below the critical temperature T_{crit} , the heat capacity, mean magnetisation, magnetic susceptibility and the correlation length of the magnetic material scales as (Equations 33.1, 33.2, 33.3 in [1])

$$\begin{aligned} c_v(T) &\sim |T_{crit} - T|^{-\alpha} \\ \langle \vec{m}(T) \rangle &\sim (T - T_{crit})^\beta \\ \chi(T) &\sim (T - T_{crit})^\gamma \\ \xi(T) &\sim |T_{crit} - T|^{-\nu} \end{aligned}$$

For calculations on a finite lattice, the correlation length $\xi(T)$ would be proportional to the size of the lattice point at the critical temperature T_{crit} . Therefore, for $T < T_{crit}$,

$$\begin{aligned} \xi(T) &\sim |T_{crit} - T|^{-\nu} \propto L \\ |T_{crit} - T|^{-\nu} &\propto L^{-\frac{1}{\nu}} \\ c_v(T) &\sim |T_{crit} - T|^{-\alpha} \propto L^{\frac{\alpha}{\nu}} \\ \langle \vec{m}(T) \rangle &\sim (T - T_{crit})^\beta \propto L^{-\frac{\beta}{\nu}} \\ \chi(T) &\sim (T - T_{crit})^\gamma \propto L^{-\frac{\gamma}{\nu}} \end{aligned}$$

Taking a logarithm of the equations, the power laws would be transformed into the form of a straight line, which could be fit to the data obtained to obtain the best estimates on the critical exponents.

- The spins become aligned to a particular direction as $T \rightarrow T_c$, the correlation between spin increases. The spins propagate their correlation over large distances despite the interaction being limited to the nearest neighbours only. The distribution of the directions of the spins will be plotted to show the ordered state below T_{crit} .
- Test simulations would be run in two dimensional systems to verify if a phase transition occurs.

3.1 Heisenberg Model

3.1.1 Hamiltonian

The Heisenberg model is the simplest model for ferromagnetic and anti-ferromagnetic solids for which the Hamiltonian is (Equation 33.4 in [1])

$$\hat{H} = -\frac{1}{2} \sum_{i,j} J_{ij} \mathbf{S}_i \cdot \mathbf{S}_j$$

where J is the coupling constant to quantify the strength of interaction between spins. If $J > 0$, then a configuration with neighbouring spins that are aligned has a lower energy. Assuming a nearest neighbour interaction with constant coupling

$$J_{ij} = \begin{cases} J & , \text{if } i \text{ and } j \text{ are neighbours} \\ 0 & , \text{otherwise} \end{cases}$$

due to which the Hamiltonian is simplified to

$$\hat{H} = -J \sum_{\langle i,j \rangle} \mathbf{S}_i \cdot \mathbf{S}_j$$

where $\langle i,j \rangle$ denotes the possible combinations of nearest neighbours. The Heisenberg model is the generalisation of the classical Ising model in three-dimensions. If an external magnetic field is present, then the interaction with the external field \mathbf{B} is taken care of by introducing a term $\sum_i \mathbf{B} \cdot \mathbf{S}_i$ in the Hamiltonian.

3.1.2 Simulation Parameters

To simulate the behaviour of spin- $\frac{1}{2}$ particles, a simple cubic lattice of $L = 12, 16, 20$ spins per side have been taken with the temperature in the range $T \in [0.50, 3.0]$ with a measurement taken every 0.1 unit of temperature. Measurements every 0.005 units of temperature have been taken in the range [1.4, 1.5], in the vicinity of the critical point. The value of $J = 1$ was taken for the simulations. Each run of the Monte Carlo taking N steps generates a set of configurations $\{c_1, c_2, c_3, \dots, c_N\}$, with the equilibrium value of an observable as

$$\langle \Theta \rangle = \frac{1}{N} \sum_{i=1}^N f(c_i)$$

Since all the configurations generated, c_i , are not statistically independent, it is possible to replace the summation over the set $\{c_1, c_2, c_3, \dots, c_N\}$ by the summation over a subset $\{c_1, c_2, c_3, \dots, c_M\}$, where $M < N$ and the elements of the set are uncorrelated, without losing accuracy, whenever the computation of the function $f(c_i)$ is computationally and time expensive. To estimate the correlation time, a trial simulation is performed and the time correlation function, $c(t)$, is plotted as a function of the number of steps taken.

$$c(t) = \langle \vec{s}(0) \cdot \vec{s}(t) \rangle - \langle \vec{s}(0) \rangle \cdot \langle \vec{s}(t) \rangle$$

For each simulation, 1×10^7 Monte Carlo steps have been taken. Measurements were started after 5×10^6 steps, by which time the system has reached equilibrium. For the case of current simulations, the measurements have been taken every 0.5×10^4 steps. The Monte Carlo algorithm is outlined in [Algorithm](#).

Algorithm :

1. Generate an initial state with energy E_0 by starting at a random configuration of the lattice (warm start, better for simulating higher temperatures) or all the spins aligned in the same direction (cold start, for simulating lower temperatures).
2. The initial configuration is changed by perturbing a spin and the energy of the trial state, E' , is calculated. As described in [6], a random mirror plane is chosen at a random lattice site and the spin at that lattice site is reflected about the chosen mirror plane.
3. Calculate $\Delta E = E' - E_0$.
4. If $\Delta E < 0$, the new configuration is accepted. (The energy has decreased and the simulation might be moving towards the global energy minima at that temperature). Proceed to step 6.
5. If $\Delta E > 0$, evaluate $p = e^{\beta \Delta E}$.
6. Generate a random number $q \in [0, 1]$. If $q \leq p$, the new configuration is accepted. Else, the old configuration is retained.
7. The steps 2 through 6 are iterated over for a sufficiently good sampling of the phase space.

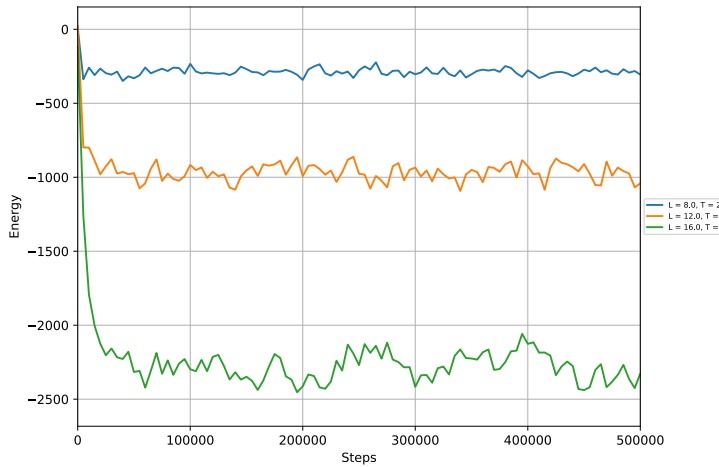


Figure 1: Trial run of the Monte Carlo with $L = 8, 12, 16$ and $T = 2.0$ to determine the validity of the chosen time for the system to reach equilibrium.

3.1.3 Implementation Details

The program for simulating a three-dimensional Heisenberg model is written in [Python 3.9.7](#), with the [Numpy](#) library used for storing matrices. Numpy has also been chosen because of its compatibility with the python package [Numba](#) which has been used to produce [JIT](#) compiled code to fasten up critical methods of the program. The results of the simulations are analysed using [Jupyter Notebook](#).

The program `set_simulation.py` provides the wrapper for the entire implementation. The script `read_config.py` reads the initial condition and simulation parameters from the passed file (`config.json` in this case). The file `simulation.py` instantiates an object of the class `TSSimulation` which runs the entire Monte Carlo simulation of an object of the class `SpinSystem` in `spin_system.py`. The usage for initialisation of a spin system is

```
\$ python ./set_simulation.py -i <simulation_name> -L <array_lengths>
-T <array\temperature>
```

and running Monte Carlo on that initialised set is

```
\$ python ./set_simulation.py -r <simulation_name>
```

A simulation directory will be created named `./simulations` with a directory with the same name as `<simulation_name>` containing the results of the simulations. The name of the directory with the results of the simulations have to be specified in the Jupyter notebook, for the loading of the results of the simulations for analysis along with the `data_analysis.py` file. The plots generated are stored in the directory `./plots/<simulation_name>/`.

3.1.4 Results

As seen from a plot of the mean energy of the system against the number of Monte Carlo steps taken, Figure 2, the system has reached equilibrium by 0.5×10^7 steps and measurements are performed after that.

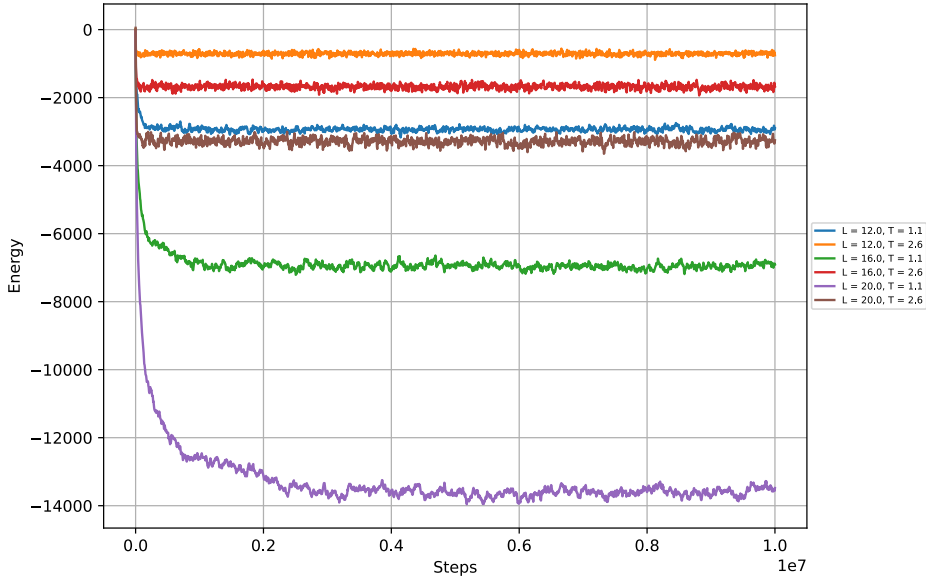


Figure 2: Variation of the Energy of the system, $\langle E \rangle$, with the number of steps taken

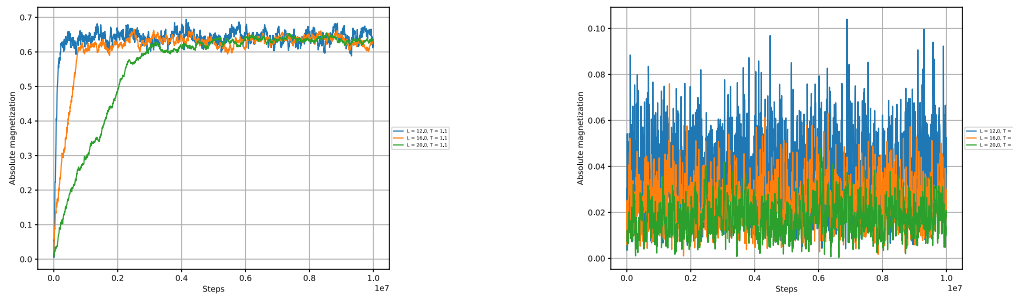


Figure 3: (Left) Variation of the magnetisation of the system with the number of steps in the ordered state (below T_{crit} , a net magnetisation, $\langle \vec{m} \rangle$, is present), and (Right) variation of the magnetisation of the system with the number of steps in the disordered state (above T_{crit} , there is negligible net magnetisation)

The magnetisation of the system is plotted as a function of the number of steps taken in Figure 3. As it can be seen from the Figure, the system undergoes a phase transition. Below a certain T_{crit} , the system exhibits an ordered behaviour with a significant value of spontaneous magnetisation while above T_{crit} , it undergoes a *phase transition* and the magnetisation is lower. The absolute values of the individual components of the magnetisation in each direction, $|M_i|$, has been plotted in Figure 4.

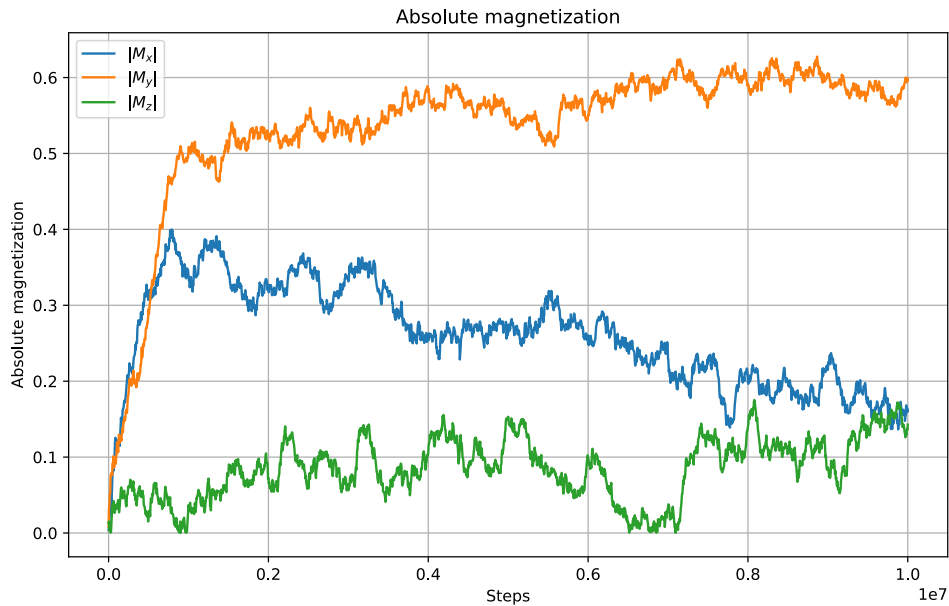


Figure 4: The absolute magnitude of the x , y and z -components of magnetisation of the system in the ordered state

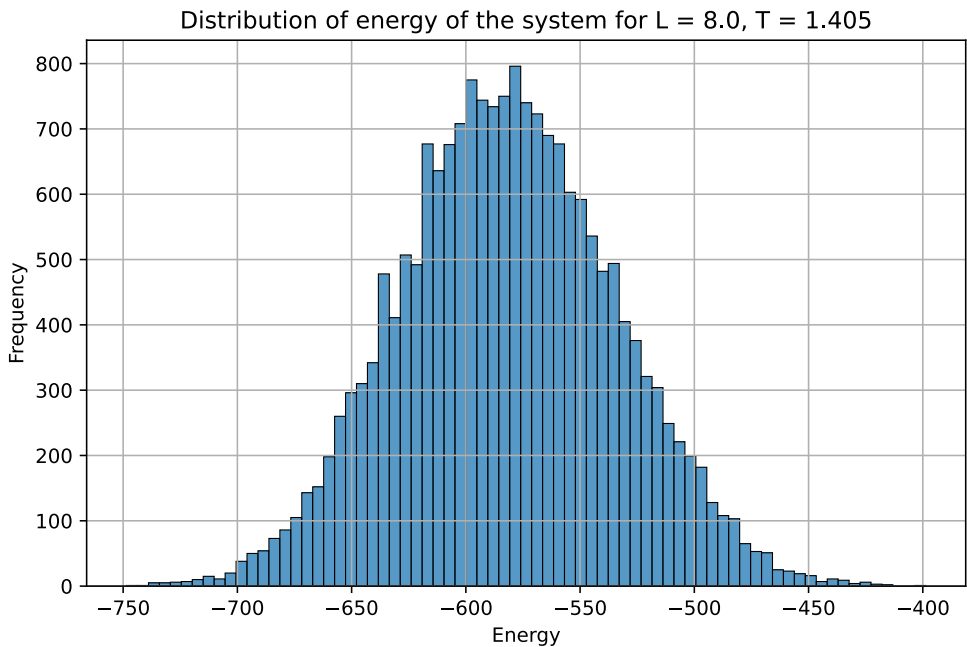


Figure 5: Distribution of the Energy of the system

The statistical distribution of the energy of the system at equilibrium (to the first order) should be a Gaussian distribution with mean as the mean energy of the system and the variance as the

heat capacity of the system, which is plotted in Figure 5. As $T \rightarrow T_c$, the distribution broadens.

In Figure 6 the energy of the system $E_L(T)$ and the energy of a single spin $E_L(T)/N$ has been plotted. $E_L(T)/N$ are the same for the same value of T irrespective of the size of the lattice, which is what is expected.

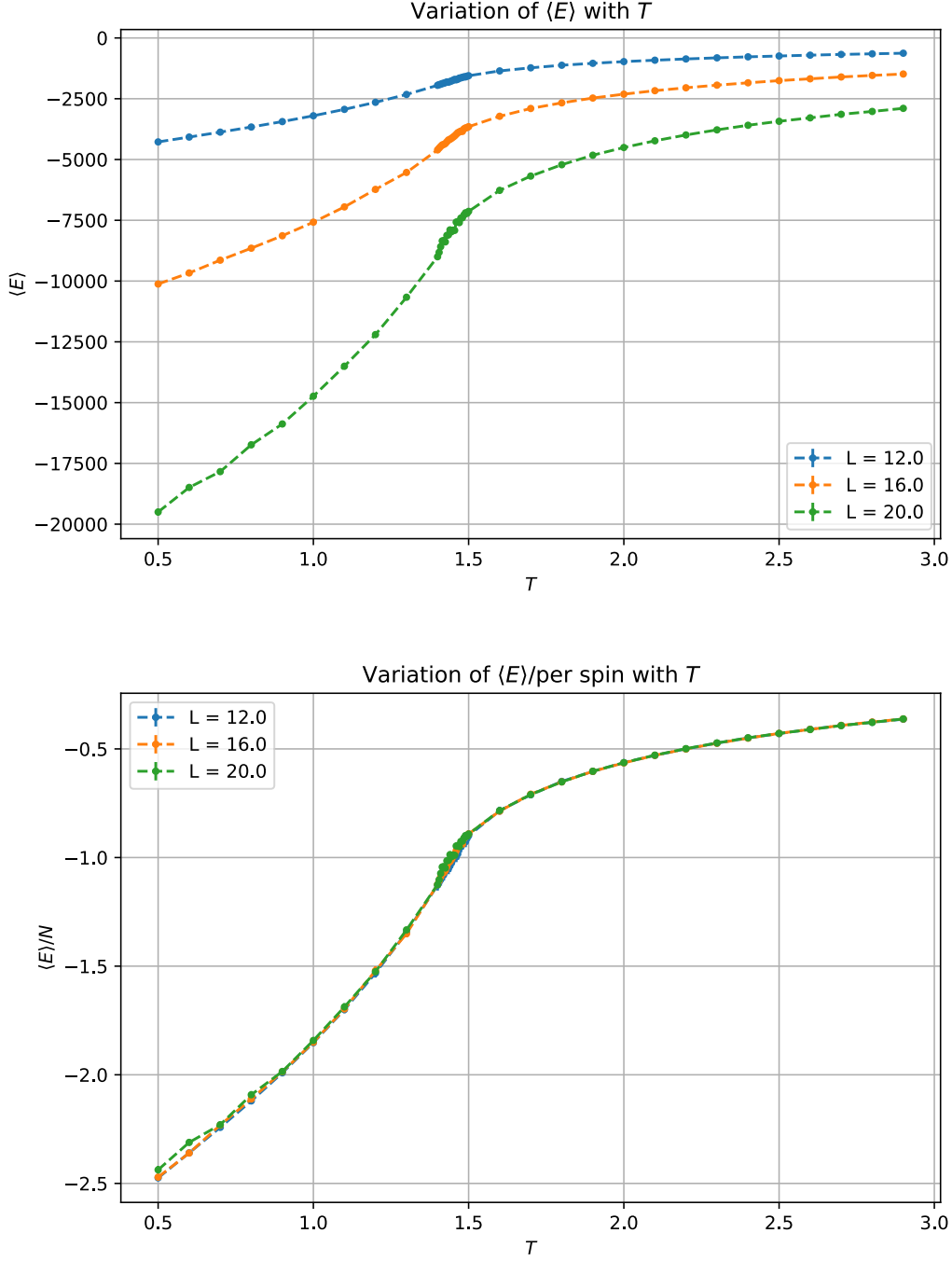


Figure 6: (Top) Expectation value of the Energy of the system as a function of the temperature. (Bottom) Expectation value of the Energy per spin as a function of the temperature.

From statistical physics, the heat capacity of the system is

$$c_v(T) = \frac{1}{N} \frac{\langle E^2 \rangle - \langle E \rangle^2}{k_b T}$$

where T is the temperature at which the heat capacity is to be measured, $N(= l^3$ for the case of a half-filled lattice) is the number of spins in the system. The heat capacity of the system has been

plotted in Figure 7 taking $k_b = 1$. The plot of $c_v T$ vs. T shows a discontinuity around $T \sim 1.4$, which is an indication of the system undergoing a phase transition around that temperature. The cusp offers a guess on the critical temperature of the system, T_c , around which samples are taken in finer intervals of temperature.

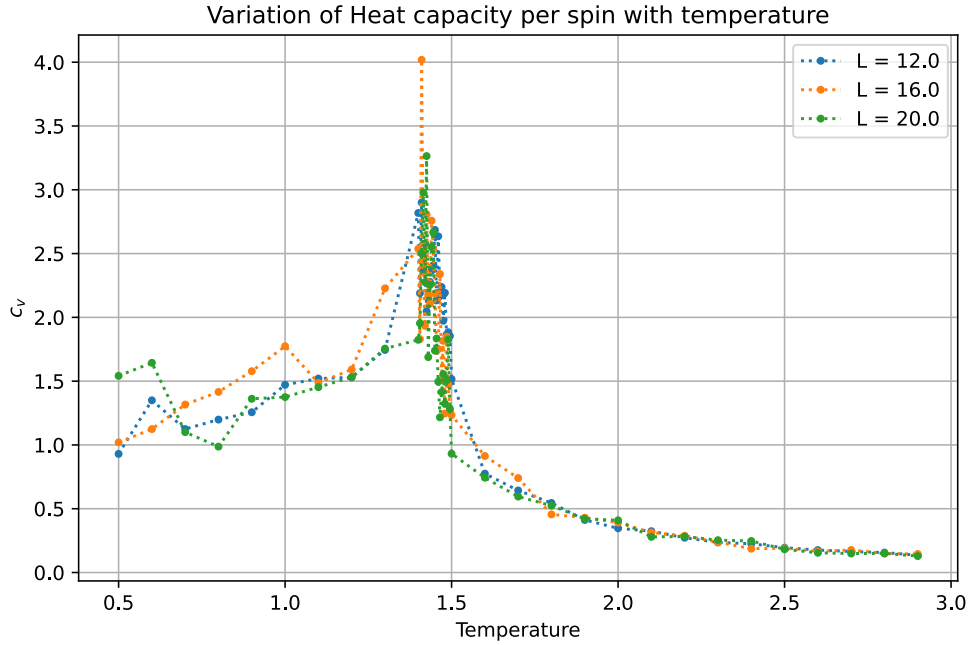


Figure 7: Heat Capacity of the system as a function of temperature

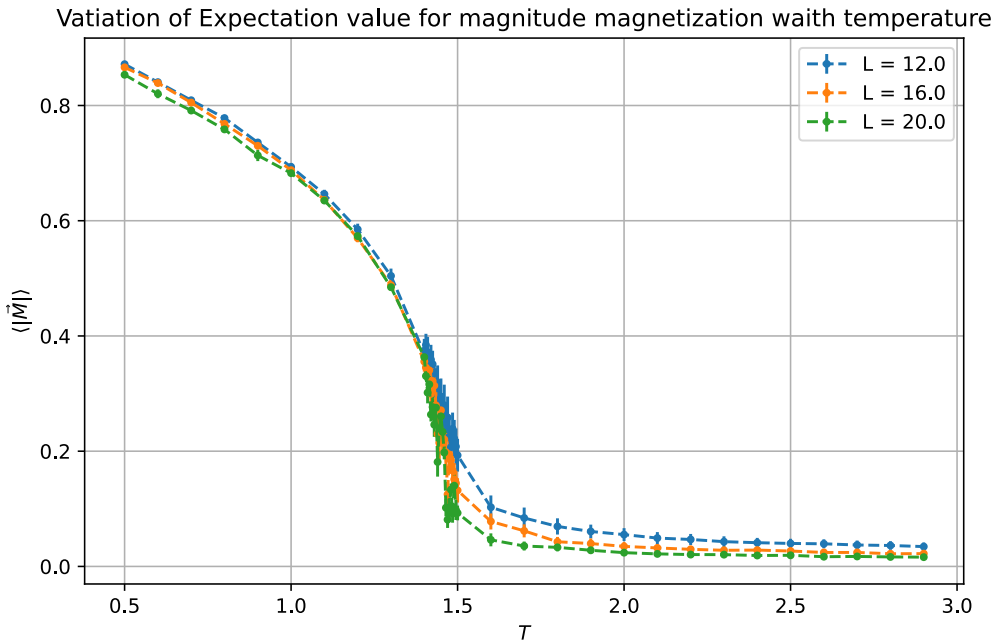


Figure 8: Heat Capacity of the system as a function of temperature

Plotting the magnetisation of the system against temperature in Figure 8, the value of magnetisation is high before the phase transition (ordered state) while it drops abruptly after the phase transition (corresponding to a disordered arrangement of the spins in the lattice). The nature of

phase transition as a second order phase transition is confirmed by Figure 8 where the magnetisation per unit spin does not show a discontinuity near the critical temperature.

The heat capacity at low temperatures converges to $c_v(T) \sim 1$ which is what it should be expected from the equipartition theorem. At each lattice, there can be two possible values of the spin, therefore two degrees of freedom.

$$\begin{aligned} c_v &= \frac{1}{N} \frac{\partial E}{\partial T} \\ &= \frac{1}{N} \frac{d}{dT} \left(2 \times \frac{1}{2} N k_b T \right) \\ &= \frac{1}{N} (N k_b) \\ &= k_b \end{aligned}$$

Lastly, a visualisation of the alignment of the spins of the system is plotted in Figures 9 and 10.

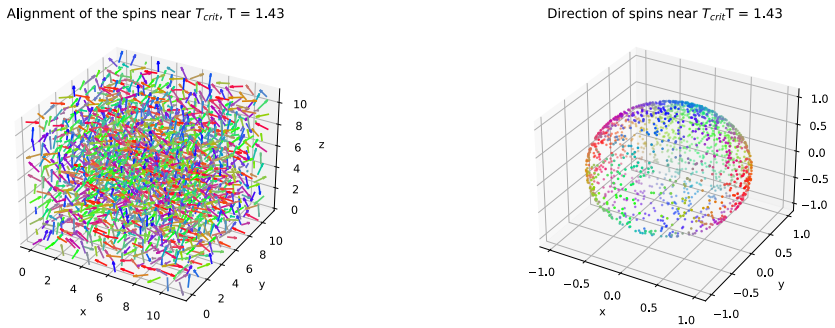


Figure 9: (Left) Alignment of the spins at the disordered state (Right) The directions of the spins are more isotropically distributed.

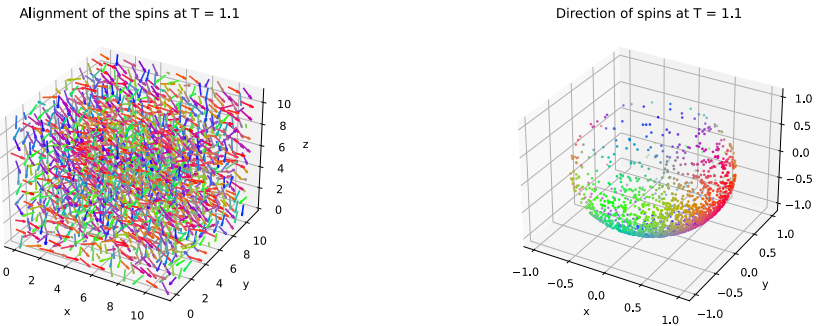


Figure 10: (Left) Alignment of the spins at the ordered state (Right) The directions of the spins have a preferential alignment.

The susceptibility of the system is given by [6]

$$\chi = \lim_{L \rightarrow \infty} \frac{L^3}{k_b T} (\langle m^2 \rangle - \langle m \rangle^2)$$

which at high temperatures reduces to

$$\chi \rightarrow \frac{L^3}{k_b T} \langle m^2 \rangle$$

as $\langle m \rangle \rightarrow 0$. The anisotropic components of the magnetic susceptibility tensor ($\chi_{xy}, \chi_{yz}, \chi_{zx}$) rapidly approach zero as the temperature of the system rises as plotted in Figure 12.

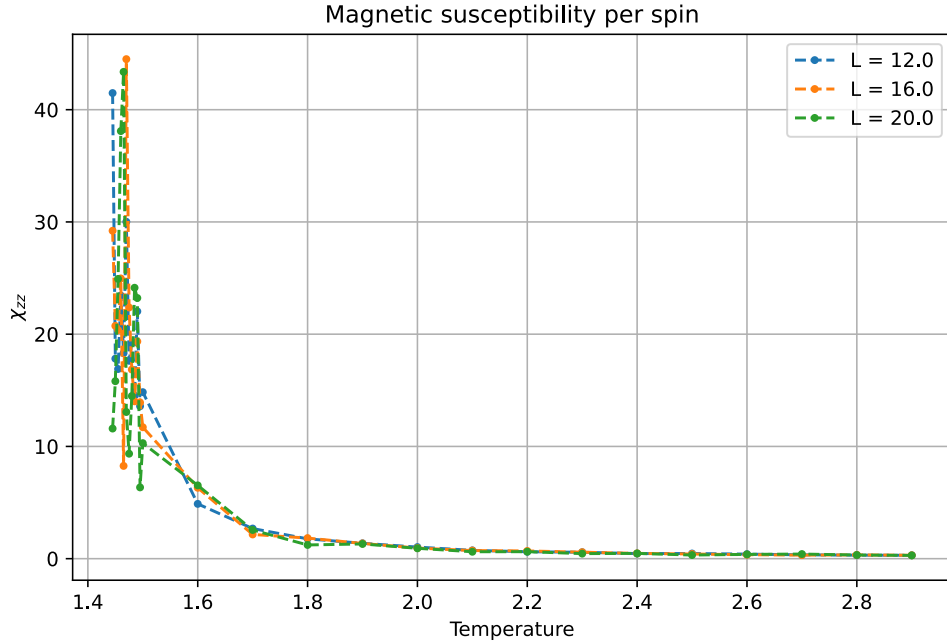


Figure 11: Magnetic susceptibility per spin in the z -direction

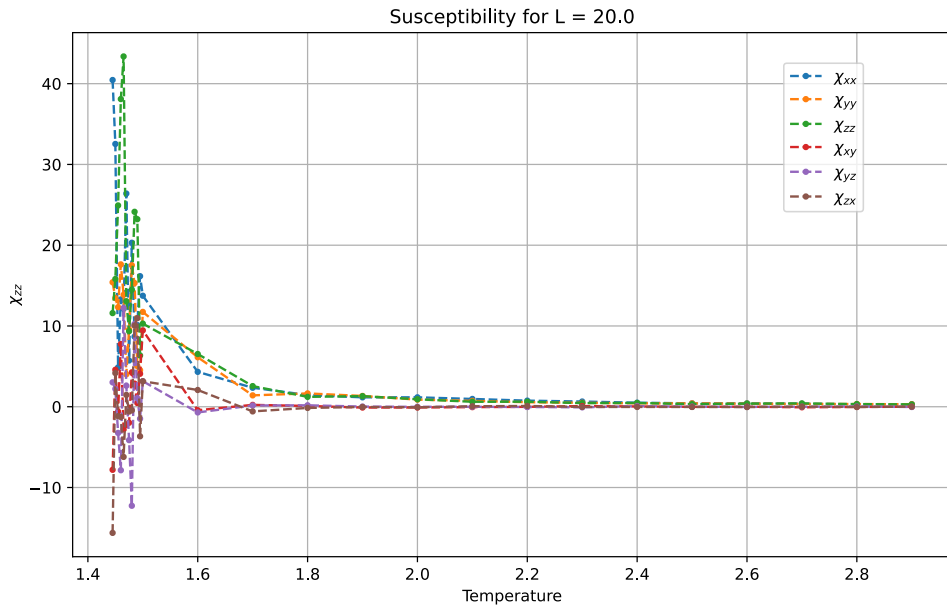


Figure 12: Elements of the Magnetic susceptibility per spin tensor

3.1.5 Determination of the Critical Temperature

$$\begin{aligned} U_L &= 1 - \frac{1}{3} \frac{\langle m^4 \rangle}{\langle m^2 \rangle^2} \\ &= \frac{2}{3} - \frac{L^6}{k_b^2 T^2} \frac{\langle m^4 \rangle - \langle m^2 \rangle^2}{3\chi^2} \\ &= \frac{2}{3} - \frac{L^6}{k_b^2 T^2} \frac{\sigma_\chi^2}{3\chi^2} \end{aligned}$$

As described in [6], the fourth order cumulant has been used to estimate the critical temperature of the system. In the limit, $T \rightarrow 0$, $\langle m \rangle \rightarrow 1$, $\langle m^4 \rangle \rightarrow 1$ and $\langle m^2 \rangle \rightarrow 1$, and hence $U_L \rightarrow \frac{2}{3}$. In the limit, $T \rightarrow \infty$, as calculated in [6], $\sigma_x^2 \rightarrow \frac{2}{3}\chi^2$ and $U_L \rightarrow \frac{2}{3} - \frac{1}{3}\frac{2}{3} = \frac{4}{9}$. These limits can also be deduced from Figure 13, the plot approaches 0.67 as $T \rightarrow 0$ and 0.44 for large T .

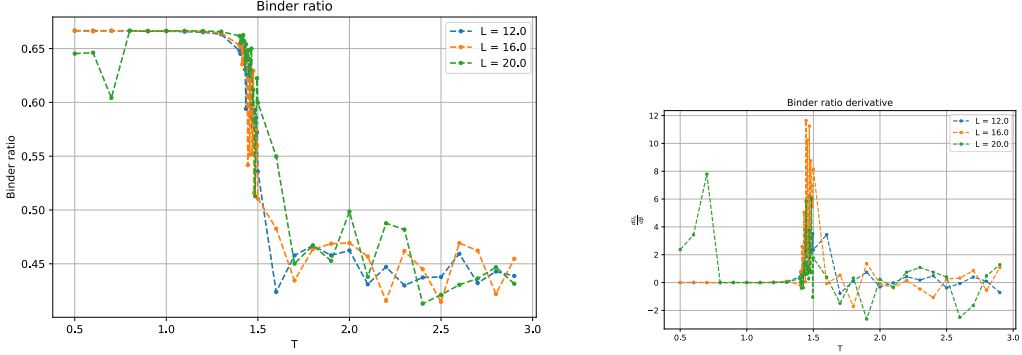


Figure 13: (Left) The value of the binder ratios for the system, (right) Derivative of the binder function

Zooming in the temperature range in the vicinity of the critical temperature, Figure 14 shows that the lines of $U_L(T)$ vs. T plot for different L intersect at $T_{crit} = 1.445$, which determines the critical temperature of the system.

Parameter	Determined value	Reference [8]	Reference [6]
T_{crit}	1.445 ± 0.005	1.4432	1.4430
β	0.6944 ± 0.0024	0.6929	0.6930

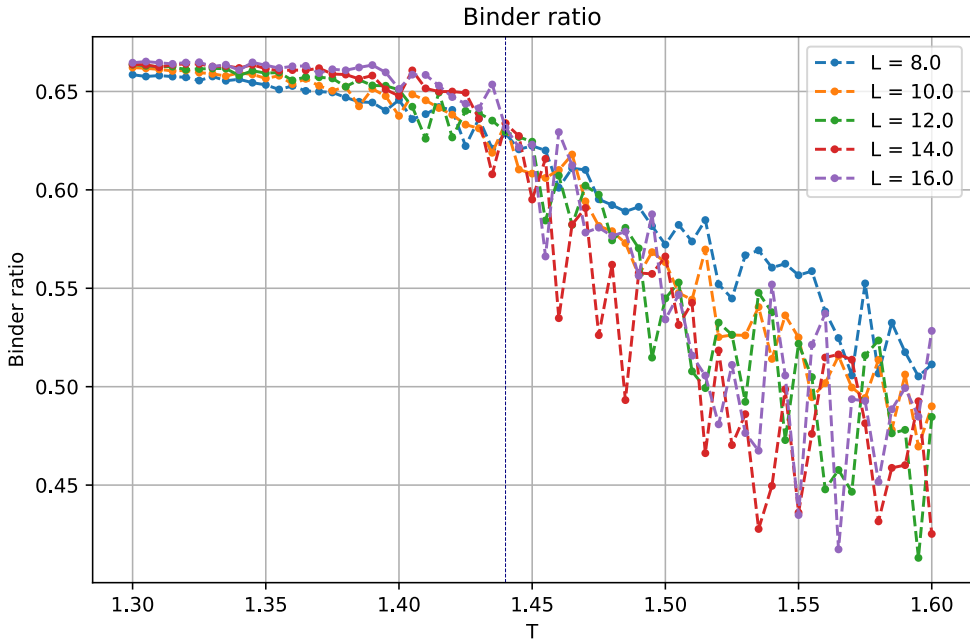


Figure 14: The value of the binder ratios for the system in the vicinity of the critical temperature, with $T_{crit} = 1.445$ shown by a vertical line.

3.1.6 Determination of the Critical Exponents

For better fits and smaller errors, the simulation parameters were altered while determining the values of the critical indices. The number of iterations was increased from 10^7 to 10^8 to decrease the errors in the Monte Carlo measurements and the size of the system was varied in the range $6 \leq L \leq 24$ in steps of 2 to obtain a larger number of data points for better estimation of the critical indices.

The magnetisation varies with the size of the system as

$$\langle m \rangle \sim L^{-\frac{\beta}{\nu}}$$

or, $\ln \langle m \rangle = c_1 - \frac{\beta}{\nu} \ln L$

Performing a χ^2 -fit between the data-sets $\ln \langle m \rangle$ and $\ln L$ would give the ratio of the critical indices β and ν .

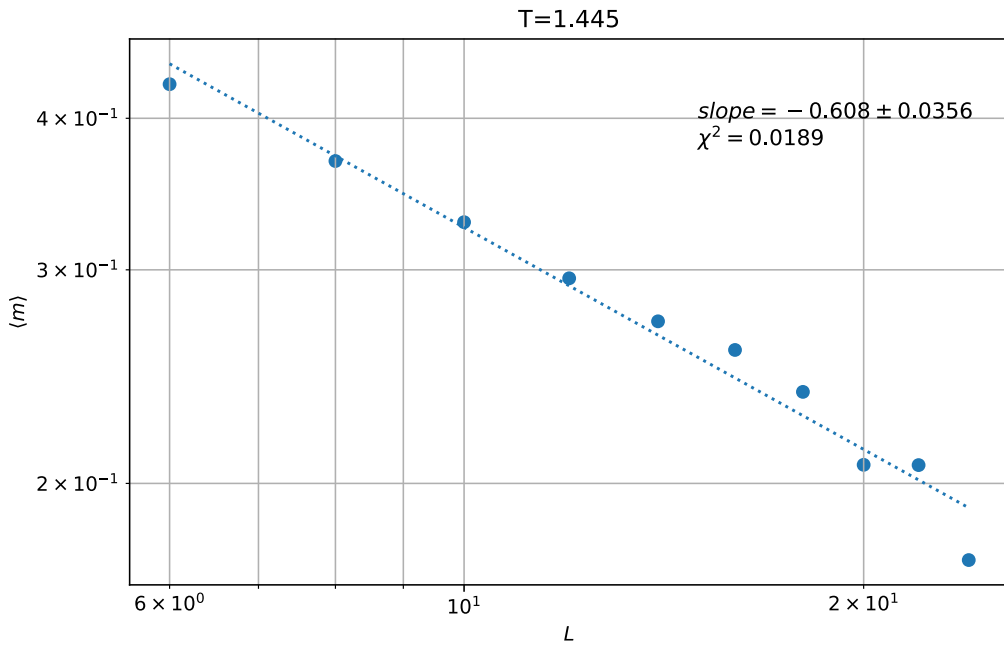


Figure 15: Log-Log plot of $\langle m \rangle$ vs L with a χ^2 -fit for the system

The magnetic susceptibility varies with the size of the system as

$$\chi \sim L^{-\frac{\gamma}{\nu}}$$

or, $\ln \chi = c_2 - \frac{\gamma}{\nu} \ln L$

Performing a χ^2 -fit between the data-sets $\ln \chi$ and $\ln L$ would give the ratio of the critical indices γ and ν .

Following Equation 54 of [2], the derivative of the fourth-order cumulant U_L around the critical point, T_{crit} , is used to estimate the value of the critical exponent ν .

$$U_L = U^* \left[1 - \left(\frac{\xi}{L} \right)^{-\frac{1}{\nu}} \pm \dots \right]$$

or, $\frac{dU_L}{d\beta} \sim L^{\frac{1}{\nu}}$

If the derivative is determined by finite-differences, then the value of the derivative is highly dependent on the interval chosen and the algorithm used (forward derivative, backward derivative

or symmetric derivative). Hence, the thermodynamic derivative is calculated following Equation 11 of [4],

$$\begin{aligned}
\frac{dU_L}{d\beta} &= \frac{d}{d\beta} \left[1 - \frac{1}{3} \frac{\langle m^4 \rangle}{\langle m^2 \rangle^2} \right] \\
&= \frac{1}{3\langle m^2 \rangle^2} \left[-\frac{d\langle m^4 \rangle}{d\beta} + 2 \frac{\langle m^4 \rangle}{\langle m^2 \rangle} \frac{d\langle m^2 \rangle}{d\beta} \right] \\
&= \frac{1}{3\langle m^2 \rangle^2} \left[\langle m^4 \rangle \langle E \rangle - 2 \frac{\langle m^4 \rangle \langle m^2 E \rangle}{\langle m^2 \rangle} + \langle m^4 E \rangle \right] \\
&= \frac{\langle m^4 \rangle}{3\langle m^2 \rangle^2} \left[\langle E \rangle - 2 \frac{\langle m^2 E \rangle}{\langle m^2 \rangle} + \frac{\langle m^4 E \rangle}{\langle m^4 \rangle} \right] \\
&= (1 - U_L) \left[\langle E \rangle - 2 \frac{\langle m^2 E \rangle}{\langle m^2 \rangle} + \frac{\langle m^4 E \rangle}{\langle m^4 \rangle} \right]
\end{aligned}$$

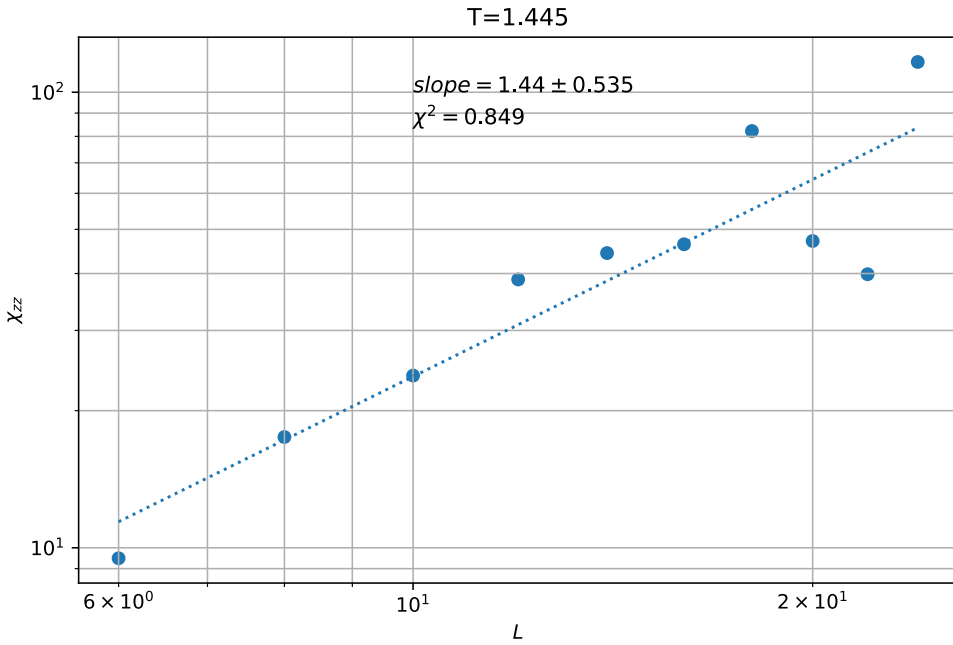


Figure 16: Log-Log plot of χ vs L with a χ^2 -fit for the system

Parameter	Determined value	Reference [8]	Reference [6]
$\frac{\beta}{\nu}$	0.60 ± 0.035	$0.516(3)$	$0.514(1)$
$\frac{\gamma}{\nu}$	1.44 ± 0.535	$1.969(7)$	—
ν	0.79 ± 0.137	$0.706(9)$	$0.704(6)$
β	0.47 ± 0.09	$0.364(7)$	$0.362(4)$
γ	1.15 ± 0.470	$1.390(23)$	$1.389(14)$
α	-0.295 ± 0.643	$-0.118(18)$	$-0.112(18)$
δ	3.363 ± 1.268	$4.819(36)$	—

Table 1: Estimates of the Critical Indices for the classical three-dimensional Heisenberg system.

The other critical exponents are determined by Equations 16.30, 16.31 from [7].

$$\begin{aligned}
\delta &= 1 + \frac{\gamma}{\beta} \\
\alpha &= 2 - \nu d
\end{aligned}$$

The estimates of the values of the critical indices and the errors are tabulated in Table 1. For most of the parameters, the values in the References [8], [6] are within one standard deviation of the estimate of the parameters from the Monte Carlo simulations.

The main source of error in the estimates is the error in the estimate of ν as the fit is the poorest in that plot. It might be due to the estimation of the derivative of the Binder ratio which involved the fourth order moment of the energy distribution and magnetisation. Calculation of the fourth order moment would require much longer simulation times and larger number of Monte Carlo steps for better convergence.

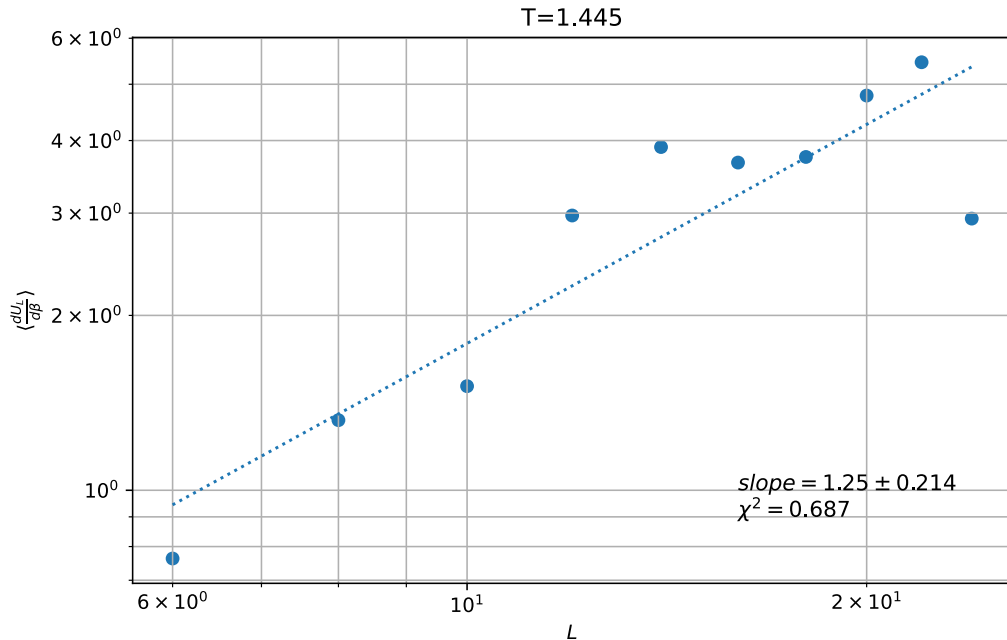


Figure 17: Log-Log plot of $\frac{dU_L}{d\beta}$ vs L with a χ^2 -fit for the system

3.1.7 Two-Dimensional Model

A two-dimensional Heisenberg model has been simulated. The anisotropic components of the magnetic susceptibility tensor ($\chi_{xy}, \chi_{yz}, \chi_{zx}$) are zero, and it can be seen more explicitly for the two dimensional case than the three dimensional case. The heat capacity is plotted in Figure 18 which has a peak in the range $T = 0.6$ to $T = 0.8$. However, there is no discontinuity here, hence there is no phase transition.

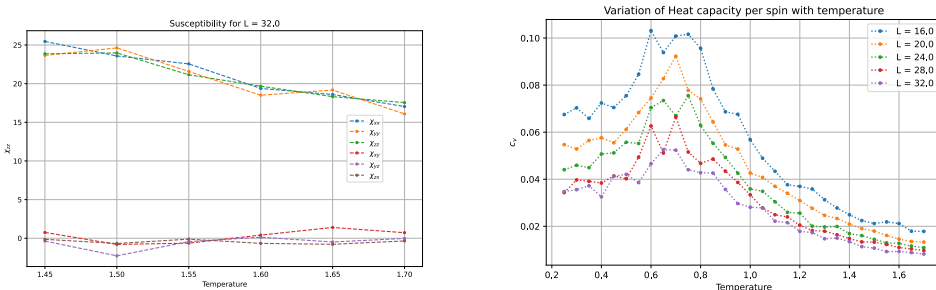


Figure 18: (Left) The components of magnetic susceptibility tensor for a two-dimensional system, (right) Heat capacities for a two-dimensional model

The plot of the Binder ratios versus temperature in Figure 19 confirm that there is no phase transition as the lines do *not* intersect each other. Figure 20 shows the state of the two dimensional system in the ordered state.

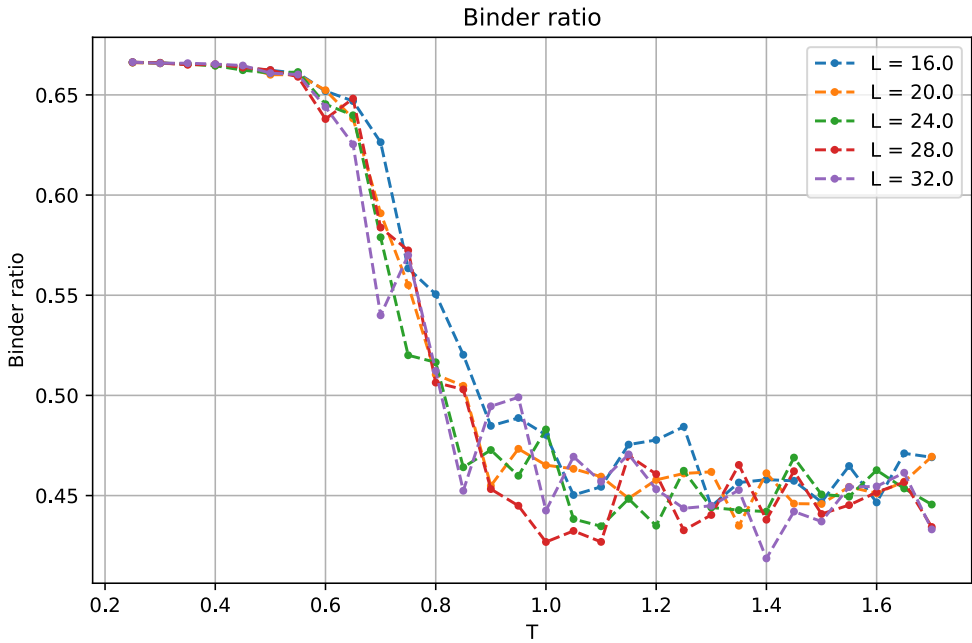


Figure 19: Binder ratio per spin for the two dimensional model

Alignment of the spins at $T = 0.25$

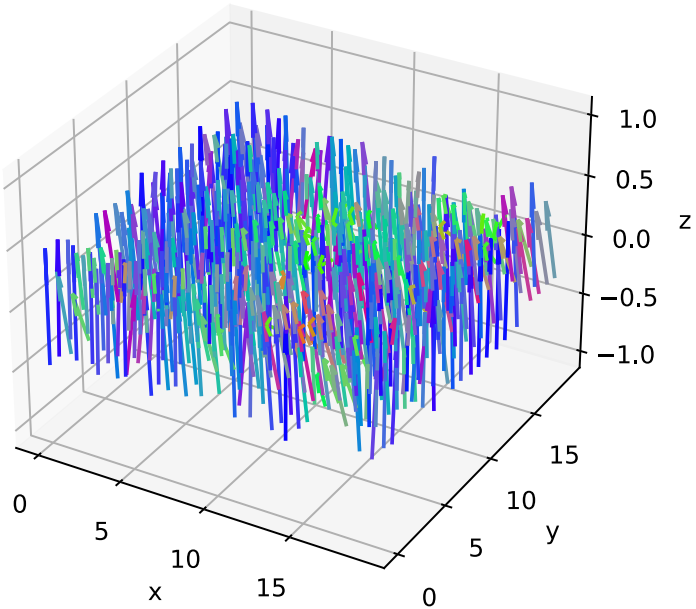


Figure 20: Ordered state of a two dimensional Heisenberg model

4 Conclusion

In this term paper, the numerical data obtained by applying Monte Carlo methods on a three-dimensional Heisenberg model (with a simple cubic lattice) has been used to determine the critical

indices of the system. The estimates are consistent with what is found in the references. The presence of phase transitions in a three-dimensional model while its absence in a two-dimensional model has also been shown.

I would like to express my sincere gratitude to the Faculty Guide for the project, Prof. V. Ravi Chandra for his guidance and time during the entire duration of the term paper. I would also like to thank the Course Instructor, Prof. Subhasis Basak for offering an opportunity to do this term paper and his helpful inputs.

References

- [1] N. W. Ashcroft and N. D. Mermin. *Solid State Physics*. Holt-Saunders, 1976.
- [2] K. Binder. [Finite size scaling analysis of Ising model block distribution functions](#). *Z. Physik B - Condensed Matter*, 43:119–140, Jun 1981.
- [3] Kurt Binder. [Monte Carlo Methods in Statistical Physics](#). Topics in Current Physics. Springer, Berlin, Heidelberg, 1986.
- [4] Alan M. Ferrenberg and D. P. Landau. [Critical behaviour of the three-dimensional Ising model: A high-resolution Monte Carlo study](#). *Phys. Rev. B*, 44:5081–5091, Sep 1991.
- [5] M. Hjorth-Jensen. [Computational Physics](#). University of Oslo, 2015.
- [6] Christian Holm and Wolfhard Janke. [Critical exponents of the classical three-dimensional Heisenberg model: A single-cluster Monte Carlo study](#). *Phys. Rev. B*, 48(2):936–950, Jul 1993.
- [7] Kerson Huang. *Statistical Mechanics*. John Wiley & Sons, 2 edition, 1987.
- [8] P. Peczak, Alan M. Ferrenberg, and D. P. Landau. [High-accuracy Monte Carlo study of the three-dimensional classical Heisenberg ferromagnet](#). *Phys. Rev. B*, 43(7):6087–6093, Mar 1991.